Experimental and theoretical study of reflection and coherent thermal emission by a SiC grating supporting a surface-phonon polariton

J. Le Gall* and M. Olivier†

Commissariat à l'Énergie Atomique, CESTA, Boîte Postale 2, 33114 Le Barp, France

J.-J. Greffet‡

*Laboratoire d'Énergétique Moléculaire et Macroscopique: Combustion, École Centrale Paris,
Centre National de la Recherche Scientifique, Grande Voie des Vignes, 92295 Châtenay-Malabry Cedex, France*

Polarized directional reflectivity and emissivity of a SiC one-dimensional grating are studied. Measurements and calculations are performed between 10 and 11.5 μm where the real part of the permittivity of SiC is negative. Pronounced dips due to surface-phonon polariton excitations are observed in the reflectivity spectra in p polarization. Thermal emission displays peaks in the same directions and at the same particular frequencies. A comparison between theory and experiments shows a good agreement for both cases. The dispersion relation is obtained theoretically and experimentally. Finally, we discuss the spatial coherence of the monochromatic thermal emission. Indeed, it is shown that the existence of peaks of the emitted-monochromatic radiation, in particular angular directions, implies that, due to surface waves, the thermally excited field is partially spatially coherent along the interface. [S0163-1829(97)06915-4]

I. INTRODUCTION

It is well known that the radiative properties of a surface are related to the surface profile. This can be used to modify the radiative properties such as reflectivity and emissivity. The presence of microcavities can increase the absorptivity of a surface. This can be understood on the basis of geometrical optics for grooves that are large compared to the wavelength (see Refs. 1 and 2). In this paper, we shall focus on the analysis of the radiative properties of a silicon carbide (SiC) grating. This material is very interesting since its dielectric constant has a negative real part for wavelengths close to 10 μm. Thus, it can support a surface wave known as surface phonon polariton (SPP). The interplay between the surface profile and the surface wave introduces large modifications of the radiative properties. A striking effect is that thermal emission displays peaks in well-defined directions and particular frequencies. This effect has been first observed by Hesketh, Zemel, and Gebhart[3] on a silicon grating supporting a surface-plasmon polariton. Up to now a quantitative description of this effect has not been given due to the difficulties of modeling the behavior of a surface wave on a deep grating. In this work we investigate in detail the thermal emission of such a grating and we fully discuss the coherence of the thermally emitted radiation. To this aim, it is necessary to analyze the behavior of the surface-phonon polariton on a grating using a numerical technique that allows one to model such a problem.

The physics of surface polaritons has been widely studied in the literature and several reviews are available.[4–6] The main experimental tool used for these applications has been attenuated total internal reflection (ATR). From experimental data it is possible to measure the dispersion relations of the surface waves. The effect of the surface topography has been studied both for gratings and random rough surfaces. Yet, despite the large amount of work on these collective excitations, there have been comparatively few experimental results reported on thermal emission. Vinogradov has given an overview of this topic.[7] Most of the results were obtained by using prisms to couple the thermally emitted surface waves to propagating waves. More recently, in a series of papers, the group at University of Pennsylvania has reported the first emission spectra obtained with a silicon grating. They have found very interesting angular and spectral behavior for both doped and undoped samples.[8–11] Yet, to our knowledge, a quantitative analysis of the results remains to be done.

The analysis of optical properties of surfaces with subwavelength structures is a rather difficult problem. A good account of theoretical techniques can be found in Ref. 12. Since Ref. 12 was published, the numerical techniques have been improved and lamellar metallic gratings with deep grooves can be handled with different techniques (see Ref. 13–15). It is worth mentioning that most of the reported work deals with the study of reflectivity. Although there is a simple link between emission and absorption given by Kirchhoff's law, there is still a lack of detailed analysis of the emission processes in the framework of electromagnetic theory. It is also of interest to note that the theoretical studies of the dispersion relation of surface wave propagating on gratings or rough surfaces have been done within the framework of perturbation theory[16] or using the Raleigh hypothesis.[17] Hence they were limited to slightly rough surfaces. An attempt to use the rigorous coupled wave theory to interpret the data obtained for deep lamellar gratings has succeeded in providing a qualitative analysis of the emission peaks.[10]

The issue of thermal emission by gratings supporting surface waves is still a challenging problem. More specifically, (i) the dispersion relation of the surface wave has to be constructed in order to fully understand the emission spectra, (ii) a quantitative comparison with a numerical technique is still lacking, (iii) the coherence of the emission and its link with

the presence of a surface wave remains an open problem.

In this paper we shall report an investigation of the radiative properties of a SiC grating. The next section is devoted to a summary of surface-phonon polariton properties. The dispersion relation on a grating will be described and the effect of losses will be discussed. The fabrication and characterization of the sample is described in Sec. III. We present in Sec. IV an experimental study of the sample. We have measured the monochromatic absorptivity at fixed wavelength as a function of the angle of incidence. We have also studied the reflectivity and emission spectra at fixed angle. From these results, we are able to construct the dispersion relation. The results are compared to theoretical results obtained by means of a volume integral equation. Finally, we discuss the issue of coherence for thermally emitted radiation.

II. SURFACE POLARITONS ON A PLANE SURFACE

A. Surface waves at a crystal-air interface

The aim of this section is to introduce the basic concepts that are necessary to interpret the resonances observed in the emission, absorption, and reflection spectra. The remarkable features of the spectra are due to the excitation of surface waves. We shall first deal with the dispersion relation of a surface-phonon polariton along a flat interface separating air from a lossy crystal. Then we shall present the modifications introduced by the presence of a grating. Finally, we shall discuss the use of the dispersion relation to interpret the spectral measurements.

In this paper we are interested in SiC. This is a lossy, linear, isotropic material that can be fully characterized by its complex dielectric constant $\varepsilon(\omega)$. It can be shown[18,19] that the dispersion relation of a SPP propagating on a flat interface can be written in the form

$$k_\parallel^2 = \frac{\omega^2}{c^2}\left(\frac{\varepsilon}{\varepsilon+1}\right), \qquad (2.1)$$

where $k_\parallel$ is the wave vector of the surface mode. The form of the dielectric constant for a crystal obtained by using an oscillator model is

$$\varepsilon(\omega) = \varepsilon_\infty\left[1 + \frac{\omega_L^2 - \omega_T^2}{\omega_T^2 - \omega^2 + i\Gamma\omega}\right], \qquad (2.2)$$

where ε_∞ is the permittivity for high frequencies, ω_T the frequency of the transverse optical phonon, ω_L the frequency of the longitudinal optical phonon, and Γ the damping. For a monocrystal of SiC, Spitzer, Kleinman, and Walsh[20] have fitted the experimental data with this expression. They have found $\omega_L = 969$ cm^{-1}, $\omega_T = 793$ cm^{-1}, $\Gamma = 4.76$ cm^{-1}, and $\varepsilon_\infty = 6.7$.

Using Eqs. (2.1) and (2.2), it is straightforward to find the dispersion relation for a nonlossy material. The problem is not so obvious when dealing with a lossy material. Indeed, no solution of Eq. (2.1) can be found if both $k_\parallel$ and ω are assumed to be real. Conversely, if both $k_\parallel$ and ω are assumed to be complex, there are four unknowns and only two equations. Thus some further *a priori* information has to be used when solving Eq. (2.1). This is based on the analysis of the physical situation that is considered. Let us first consider the
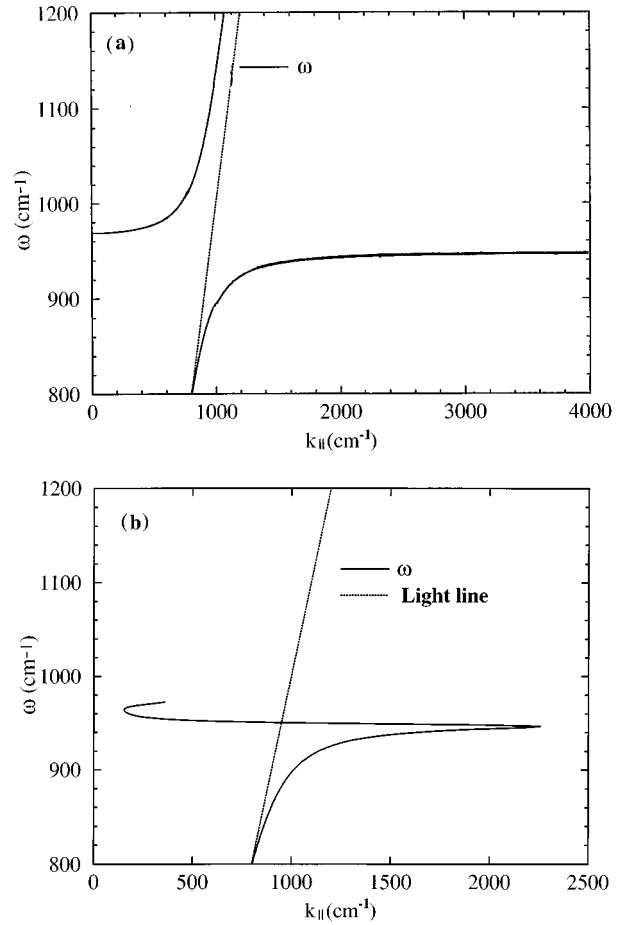

FIG. 1. Dispersion relation of a surface-phonon polariton on a plane surface. (a) Case where $k_\parallel$ is assumed to be real. (b) Case where ω is assumed to be real.

case of a measurement made at constant angle of incidence and varying the frequency (e.g., an ATR spectrum or an emission spectrum). If a surface mode is excited, a peak may appear for a given frequency and with a given width. It turns out that the position of the frequency gives the real part of the mode frequency whereas the width of the peak provides the imaginary part of the frequency. The incident angle yields the (real) wave vector. Thus it appears that such a frequency spectrum can be well described by assuming that the frequency is complex and the wave vector is real. For many years this has been the standard way of interpreting ATR spectra. The dispersion relation is depicted in Fig. 1(a). One can see two distinct branches. In fact, the upper branch does not describe a guided mode since it lies in the light cone. The lower branch is always below the light line and describes a true surface mode. Note that the frequency tends asymptotically to ω_{sup} for large values of the wave vector where ω_{sup} is defined by

$$\omega_{\text{sup}} = \left(\frac{\varepsilon_0 + 1}{\varepsilon_\infty + 1}\right)^{1/2}\omega_T \qquad (2.3)$$

in the case of a diatomic crystal when the damping is neglected (i.e., ω and $k_\parallel$ are real).[21]

An alternative choice could have been used when solving Eq. (2.1). It is possible to choose a real frequency and a
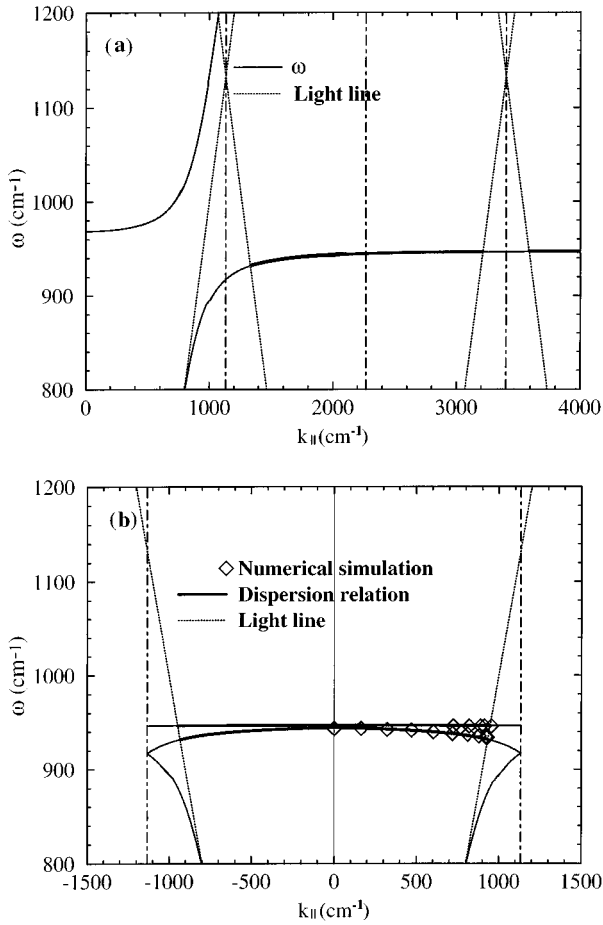
FIG. 2. Dispersion relation of a surface-phonon polariton on a smooth grating. (a) Extended zone scheme. (b) Reduced zone scheme.

complex wave vector. This choice leads to a very different dispersion relation, shown in Fig. 1(b). It is seen that a back-bending of the curve appears in the frequency region where no modes were obtained with the alternative choice. Halevi[22] has discussed the modes corresponding to a region where the real part ε' of the permittivity satisfies $\varepsilon' > -1$. This result was first considered as a mathematical curiosity until Arakawa reported experimental data obtained with a fixed frequency and varying the angle of incidence.[23] With this experimental procedure, the experimental dispersion relation also shows a back-bending. This alternative choice (complex wave vector and real frequency) is natural when a reflection spectrum is presented as a function of the wave vector. The peak position provides the real part of the wave vector whereas its width provides its imaginary part. The reader can find further discussion of this point by Kliewer and Fuchs[24] and Halevi.[22]

B. Excitation of surface polaritons by a grating

As shown in Fig. 1(a), surface polaritons are nonradiative modes; i.e., they cannot be radiated as photons and cannot couple with light in conventional experiments. In the presence of a grating, surface polaritons will become radiative due to their interaction with the periodic profile. In Fig. 2(a), a set of curves corresponding to the light cone translated by

$2\pi m/a$ is shown. The period of the grating is equal to 4.41 μm. The portions of the dispersion relation that lie within the light cones correspond to surface-phonon polaritons that are able to radiate upon interaction with the periodic profile. The radiative portions of the curve are denoted by bold portions of the curve.

It is well known that the dispersion relation can be represented in an extended-zone scheme as in Fig. 2(a) or in a reduced-zone scheme as in Fig. 2(b). The large values of the wave vector that appear in the extended zone scheme Fig. 2(a) correspond to the upper branch of the dispersion relation in the reduced zone scheme as seen in Fig. 2(b). When looking at Fig. 2(a), it appears that some portions of the dispersion relation lie in the light cones. These portions of the dispersion relation lie in the light cone in the reduced zone scheme [see Fig. 2(b)]. Therefore, the corresponding SPP can be radiated by the grating. Conversely, an incident beam that necessarily lies in the light cone can excite these portions of the branch of the SPP. The portions of the dispersion relation that lie out of the light cone in the reduced zone scheme are true surface modes fully bound to the surface as discussed by Laks, Mills, and Maradudin.[16] They cannot be studied using a grating.

In order to illustrate how a grating can be used to study SPP, we performed a calculation of the reflected efficiency by a shallow sinusoidal grating, defined by $z = h \sin(2\pi x/a)$ with a half amplitude $h = 0.19$ μm and a period $a = 4.41$ μm. This calculation was based on the Rayleigh hypothesis.[27] The spectral reflectivity is obtained at a fixed angle of incidence as a function of ω. As discussed in Sec. II A, this kind of experiment (fixed angle of incidence) should be consistent with a dispersion relation of the type of Fig. 2(b). We have used the numerical experiment to build the dispersion relation in the following way. A reflectivity spectrum has pronounced dips when a SPP is excited. Thus the dips yield the frequency ω_m. The wave vector of the corresponding SPP satisfies

$$k_\parallel = \frac{\omega_m}{c} \sin\theta_i + \frac{2\pi}{a} m, \qquad (2.4)$$

where θ_i is the angle of incidence.

In the reduced-zone scheme, m is the label of the different branches, and the points have the coordinates $(\omega_m/c \sin\theta_i, \omega_m)$. This yields a point of the dispersion relation. Each fixed angle of incidence yields a point for all the branches and one wave vector. By varying the angle of incidence, it is possible to obtain the dispersion relation. We have plotted (diamonds) in Fig. 2(b) the dispersion relation as obtained with a shallow grating and the dispersion relation for a flat surface given by Eq. (2.1) obtained by assuming a complex ω and a real $k_\parallel$. Good agreement between the theoretical dispersion relation for a flat surface (plain line) and for the numerically obtained dispersion relation for the shallow grating (diamonds) is observed. Thus, the grating does not perturb significantly the dispersion relation for this particular case. The result is also in agreement with the dispersion relation given by Paulick[25] for a SPP on a shallow grating (not shown here).

Dips of reflectivity are observed when the excitation condition (2.6) is satisfied. Emission peaks also appear when this
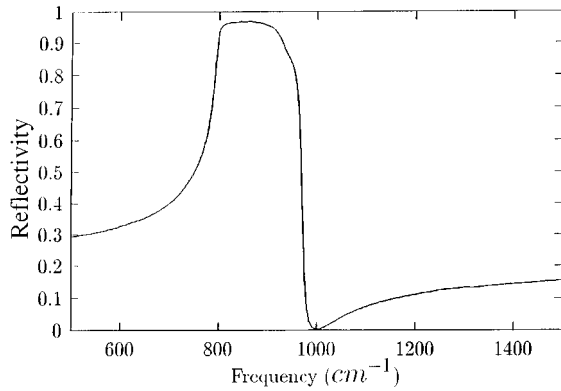
FIG. 3. Spectral reflectivity of SiC measured at near normal incidence (6°).

condition is satisfied. In what follows, we will present theoretical and experimental results of reflectivity and emissivity of a SiC lamellar grating.

III. CHARACTERIZATION OF THE SiC GRATING

A. Optical index

In all the experiments, the SiC sample used for the measurements is polycrystalline. We have checked that the polycrystal has the same behavior as a monocrystal with a dielectric constant given by Eq. (2.2). The spectral reflectivity of a sample of SiC with a flat surface was measured at an incidence of 6° (see Fig. 3). The amplitude of the reflectivity $r(\omega)$ can be written as

$$r(\omega) = \rho(\omega) \exp[i \theta(\omega)]. \tag{3.1}$$

Using the Kramers-Krönig relations we deduce $\theta(\omega)$ from $\rho(\omega)$.[26] In Fig. 4, the computed optical indexes are presented as a function of the wave number. Our results agree within $\pm 1\%$ with the oscillator model of Eq. (2.2) using the data published by Spitzer, Kleinman, and Walsh.[20]

B. Realization

The grating was fabricated on SiC by a combination of electron-beam lithography and plasma etching. A polished SiC substrate was coated with 600 nm of SiO_2 by plasma-
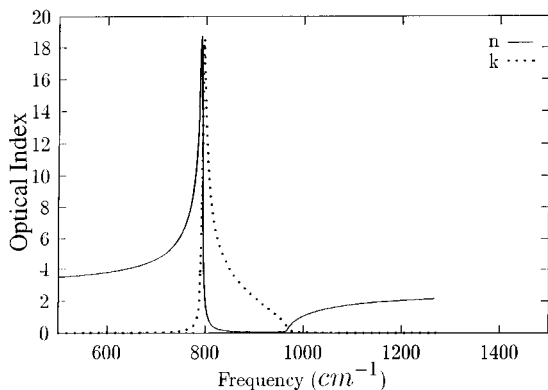

FIG. 4. Optical indexes obtained from the reflectivity data using the Kramers-Kronig relations.
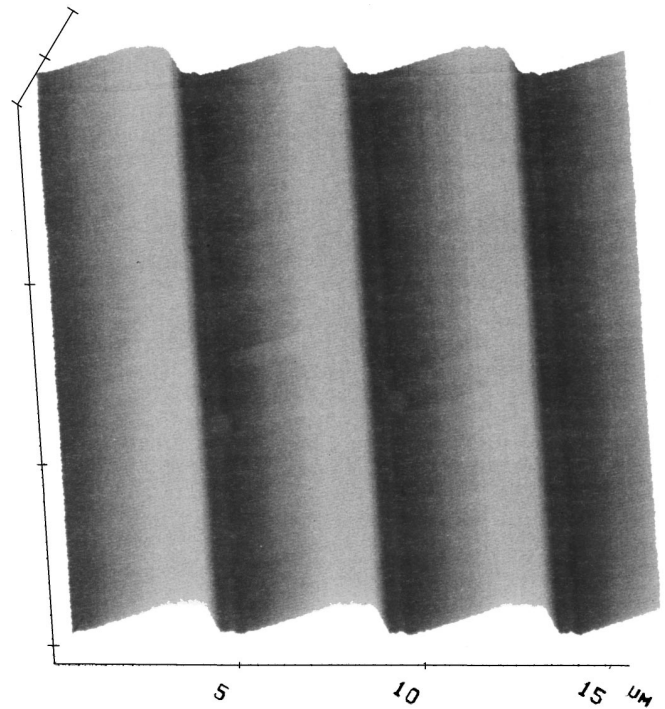

FIG. 5. Surface profile of the SiC grating measured by atomic force microscopy.

enhanced chemical vapor deposition. Then a resist layer was spin deposited on the SiO_2 and patterned with an electron-beam pattern generator. After development and stripping off of the resist, the exposed SiO_2 areas were etched in a CHF_3, O_2F_6 argon plasma. The resulting SiO_2 mask was used to pattern the SiC surface. A distributed electron cyclotron resonance plasma source was employed to etch the SiC areas. This permits anisotropic and uniform etching of the material. Finally the remaining SiO_2 mask was removed in a HF immersion. Figure 5 presents the measurement of the SiC grating surface profile using an atomic force microscope. We have obtained the following values for the depth and the width d: $h = 0.7$ μm and $a = 4.4$ μm.

IV. EXPERIMENTAL STUDY OF THE RADIATIVE PROPERTIES

A. Description of the geometry

Throughout this study, the plane of incidence defined by the normal to the interface and the direction of propagation of the incident wave is perpendicular to the lines of the grating. The electric field is depicted in Fig. 6 for p polarization. For s polarization, the electric field is perpendicular to the plane of incidence.

B. Directional absorptivity measured by mirage effect

1. Description of the experimental setup

For measuring directional absorptivity, we use a photothermal technique at variable pump angles (mirage effect). A more detailed description of the setup was presented by Le Gall et al.[28] Figure 7 is a schematic view of the experimental setup. The pump beam is a CO_2 laser, at 10.6 μm. The inci-
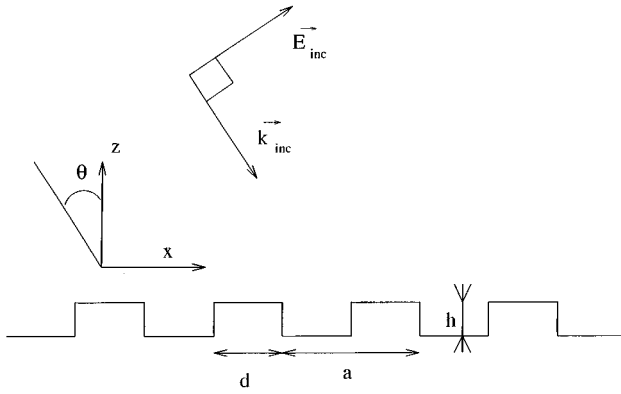
FIG. 6. Scheme of the studied system.

dent angle θ can vary between $-80°$ and $+80°$. By a combination of waves plates, the incident pump beam has a controlled polarization when impinging on the sample. Then by a two-quadrant position sensor, the photothermal deflection $D(\theta)$ of the probe beam is measured. This detector is connected to a lock-in amplifier in order to improve the signal-to-noise ratio. The absorptivity $A_{rough}(\theta)$ of a rough surface such as a grating is measured by comparing the photothermal deflections $D_{rough}(\theta)$ and $D_{smooth}(\theta)$ respectively obtained on the rough surface and on a smooth surface. The absorptivity of a rough surface $A_{rough}(\theta)$ can be written as

$$A_{rough}(\theta) = A_{Fresnel}(\theta) \frac{D_{rough}(\theta)}{D_{smooth}(\theta)}, \qquad (4.1)$$

with $A_{Fresnel}(\theta) = 1 - R_{Fresnel}(\theta)$ where $R_{Fresnel}(\theta)$, the Fresnel reflectivity, can be evaluated from the optical index.

2. Experimental results

Figure 8 shows the directional absorptivity at 10.6 μm (943 cm^{-1}) for the grating and for a plane surface for both polarizations. The measurements are performed for θ_i varying from 0° up to 80°. The directional absorptivity is larger for the grating than for the flat surface. The difference is important for p polarization. The increase of absorption for s polarization remains low. This effect can be interpreted as an absorption due to the excitation of the SPP. Yet, it is seen that the absorption is enhanced for a wide band of angles of incidence. This can be qualitatively understood upon examination of the dispersion relation in Fig. 2(b). The frequency used (943 cm^{-1}) lies in a region where the dispersion relation is almost constant. Thus, the SPP is excited for any value of $k_{\parallel}$ in the first Brillouin zone.
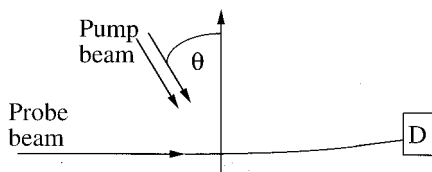

FIG. 7. Principle of the measurement of the directional absorptivity. The detector D measures the angular deviation of the probe beam (HeNe laser). The pump beam is a CO$_2$ laser ($\lambda = 10.6$ μm).
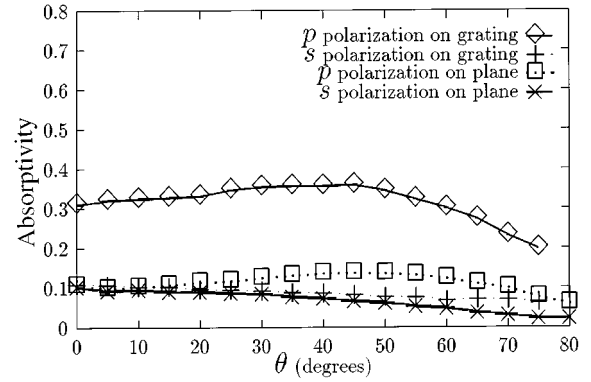

FIG. 8. Directional absorptivity measured on the SiC grating ($\lambda = 10.6$ μm).

C. Measurement of spectral reflectivity

1. Description of the experimental setup

An infrared spectrophotometer allowing a variable incident angle was specifically developed to characterize the reflectivity of the grating. Infrared monochromatic light comes from a globar coupled to a grating monochromator. The beam is then polarized by means of a grid polarizer. The sample is placed on a rotating stage. The incident angle on the sample can be varied from 6° to 80°. Detection is ensured by a photovoltaic HgCdTe unit. The detector is connected to a lock-in amplifier in order to improve the signal-to-noise ratio. The experimental setup is sketched in Fig. 9. By a combination of lenses and diaphragms, one can obtain an angular resolution of the incident beam on the sample about 1.2°. The slits of the monochromator are opened in order to obtain a spectral resolution equal to 3.5 cm^{-1}.

2. Experimental results

Figure 10 presents the spectral reflectivity in p polarization measured on the SiC grating and on a flat surface at 6° of incidence. The reflectivity is drastically modified when compared to the reflectivity of the flat surface. Three dips appear between 833 and 1000 cm^{-1}. The more pronounced
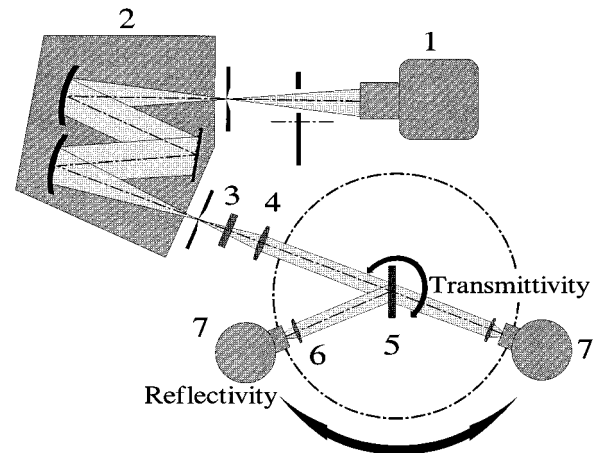

FIG. 9. Experimental setup used for measuring the spectral reflectivity. 1: IR source; 2: monochromator; 3: polarizer; 4,6: convergent lens; 5: sample, 7: IR detector.
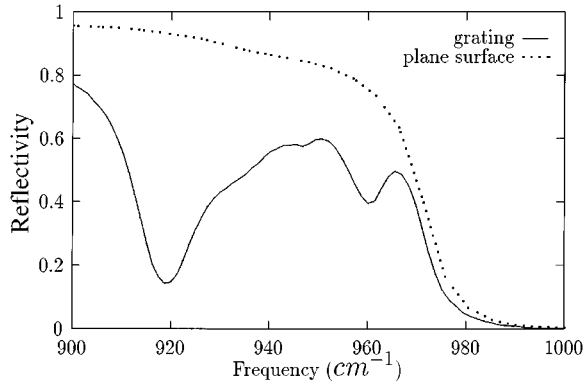
FIG. 10. Spectral reflectivity of the grating and of the plane surface for p polarization at near normal incidence ($\theta_i = 6°$).

FIG. 11. Emissivity of the SiC grating for both polarizations at near normal incidence ($\theta_i = 6°$).

one is located at 917 cm^{-1}. Another one occurs at 962 cm^{-1} and the third, which is less visible, corresponds to a wavelength of about 947 cm^{-1}. To interpret these data, we can relate them to the dispersion relation presented on Fig. 1(a) for a flat surface. It is seen that at a fixed $k_\parallel$, two branches appear providing two resonant frequencies. It is obvious that for the grating used in the experiment, the dispersion relation is significantly modified. To interpret these data, a theory that goes beyond the perturbation theory is necessary. This is the subject of Sec. V.

D. Measurement of spectral emission

1. Description of the experimental setup

We have used a third technique to study the radiative properties of the SiC grating. We have measured the fre-
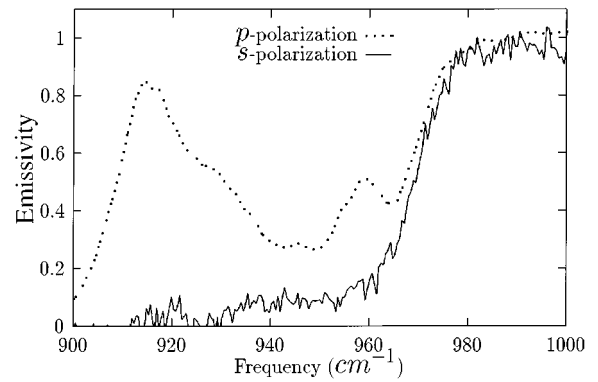
quency spectrum of the light thermally emitted at a fixed observation angle. The experimental setup described in Fig. 9 is used. In the emission configuration, the sample is the light source. Therefore, the positions of the MCT detector and the lamp are reversed. We use a halogen lamp to warm up the sample in order to increase the emitted flux Φ. The flux $\Phi_a(\theta, \lambda, \text{polar}, T_a)$ emitted by a reference sample (bore) of known emissivity is measured under the same conditions. The temperatures of both samples, T_s, T_a, respectively, are also characterized by means of an infrared camera, which allows one to control the homogeneity of the surface temperature. A number of measurements were carried out in the range $95° \leqslant T_{s,a} \leqslant 110$ °C. The background emission of the instrument $I_b(\theta, \lambda, \text{polar}, T_b)$ was measured. T_b denotes the background temperature. By combination of these processes, the absolute emission of the sample can be determined by

$$\varepsilon_s(\theta, \lambda, \text{polar}) = \varepsilon_a(\theta, \lambda, \text{polar}) \frac{I(T_a) - I(T_b)}{I(T_s) - I(T_b)} \frac{\Phi_s(\theta, \lambda, \text{polar}, T_s) - \Phi_b(\theta, \lambda, \text{polar}, T_b)}{\Phi_a(\theta, \lambda, \text{polar}, T_a) - \Phi_b(\theta, \lambda, \text{polar}, T_b)}, \quad (4.2)$$

where $I_{s,a,b}(T_{s,a,b})$ is the specific intensity of the sample, the standard, and the background, respectively, and $\varepsilon_a(\theta, \lambda, \text{polar})$ is the emission of the standard.

The angular resolution of the collected beam is equal to 6°. The angle of the flux collection can vary from 0 up to 60°. This is limited by the mechanical environment.

2. Experimental results

The curve in Fig. 11 presents the emission of the SiC grating measured for both polarizations. Light is collected at an angle of 6° from the normal to the grating. The dips observed in Fig. 10 appear in this last curve as peaks at 916, 961, and 945 cm^{-1} for p polarization.

The peaks observed on the emission measurements appear nearly at the same position as the dips observed on the reflectivity measurement. For s polarization, no similar effect was observed. The peaks of emissivity can be attributed to the emission of light due to the SPP thermally excited. Note the correlation of the positions of the dips and the peaks in

Figs. 10 and 11, respectively. Since the grating has only reflected order (zero order), we have $R + A = 1$. Kirchhoff's law[29,30] establishes that $\varepsilon = A$, thus we have $\varepsilon = 1 - R$. For this reason, Figs. 10 and 11 look similar. Yet the measurements for the reflectivity and the emission were done at different temperature of the sample.

V. EXPERIMENTAL AND THEORETICAL ANALYSIS OF THE DISPERSION RELATION

The analysis of the spectra presented above has clearly shown that the presence of dips can be explained using the dispersion relation. In order to fully characterize the radiative properties of the grating, it is therefore necessary to obtain the exact dispersion relation of the surface excitation. We will report the experimental dispersion relation obtained by the different techniques that we have used.

The theoretical description of such a system is a challenging problem. The grating is beyond the capabilities of the
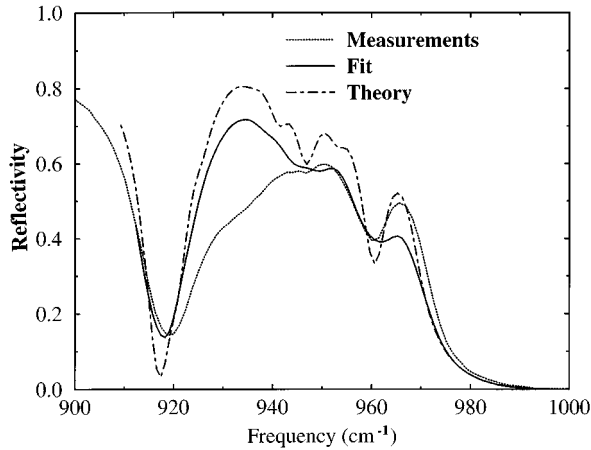
FIG. 12. Comparison between the measured and the calculated spectral reflectivity of the SiC grating at 6° of incidence.

FIG. 13. Dispersion relation of the surface-phonon polariton on a SiC grating obtained from reflectivity data.

techniques that have been traditionally used to investigate the dispersion relation of SPP along gratings (e.g., perturbation theory and techniques based on the Rayleigh assumption).[31,21,16] Wang and Zemel[10] have used the coupled wave method and have obtained only qualitative agreement with experimental data of emission by Si grating. A different technique will be used in this section to analyze this scattering problem.

Finally, we will discuss the specific problem of the thermal emission spectra in terms of coherence.

A. Numerical simulation

We have considered the scattering of a plane wave by a grating. We can simulate the reflectivity measurements of the absorption measurements since they are related by the conservation of energy relation $\varepsilon = A = 1 - R$. To simulate a scattering spectrum, we have used a volume integral equation of the Lippman-Schwinger type solved using a moment method as described in Ref. 15. This formalism is well suited to the present problem since it can handle deep gratings. In particular, the method is numerically stable in the case of negative dielectric constant and p polarization. Another advantage of this technique is that it is well suited to a lamellar grating.

B. Comparison between the measured and the calculated reflectivity

The experimental data obtained for p polarization are compared in Fig. 12 to the reflectivity obtained by the numerical simulation. The positions of the three dips agree with the experimental results. A fair agreement is obtained between the measurements and the theory. To improve the comparison, we have simulated the limited angular resolution of the data by convoluting the theoretical results with a rectangle function. When we account for this effect, the three peaks' values are in good agreement with the data. Yet the theory does not reproduce the data in the region around 935 cm^{-1}. We have checked that this could not be attributed to small errors in the grating parameters. We have not been able to explain the difference.
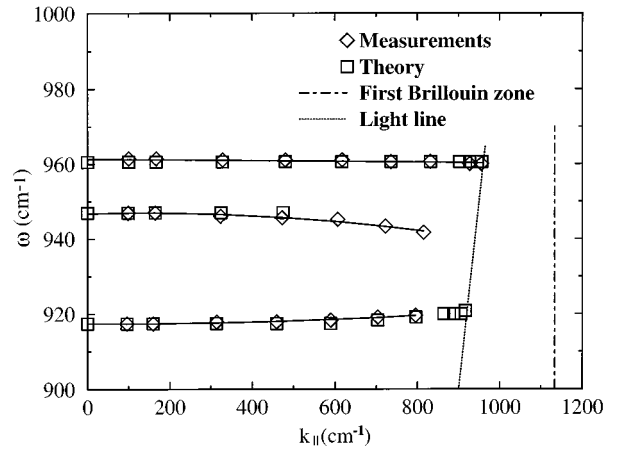
C. Dispersion relation

The procedure to determine experimentally the dispersion relation has been sketched in Sec. II. From a frequency spectrum (e.g., Figs. 8, 10, and 11) we obtain the resonance frequencies, and the corresponding wave vector in the reduced zone scheme is given by $\omega/c \sin \theta_i$. By varying the angle of incidence, we are able to scan the dispersion relation. Since our experimental setup is limited to angles lower than 60°, we have used an ellipsometer[32] to obtain data at 75° and 85°. The dispersion relation obtained from the reflectivity data is shown in Fig. 13. The points are localized in the first Brillouin zone. We have also reported the theoretical data obtained with a similar procedure (i.e., from simulated reflectivity spectra). There is a good agreement: the difference between theory and experiment does not exceed 0.1%.

The dispersion relation obtained by the numerical computation was also compared to the points deduced from the thermal emission measurements (see Fig. 14). The measurements are more difficult than for a reflectivity spectrum. The peak around 947 cm^{-1} is less visible and its spectral peak position is not easy to determine. Nevertheless, the difference between the measurements and the theory does not exceed 0.3%. A slight shift of the main peak is noticed. Indeed,
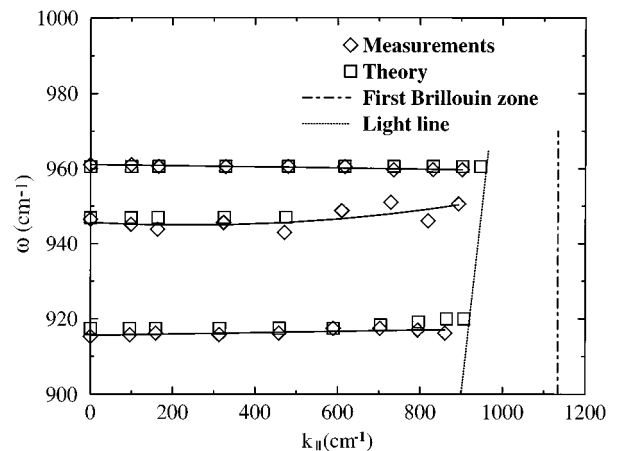

FIG. 14. Dispersion relation of the surface-phonon polariton on a SiC grating obtained from emissivity data at 100°.

the resonance occurs at 918 cm^{-1} at normal incidence and it is greater than 917 cm^{-1}, whatever the angular value. Yet, good agreement with theory should not be expected since we have used the values of the index at 300 K whereas the sample is heated at roughly 100 °C. Nevertheless, the observed shifts and the evaluation of the error is still included in the spectral resolution of our experimental setup (3.5 cm^{-1}). We attribute the discrepancy to the variation of the intrinsic properties. Similar behavior was reported by Vinogradov, Zhizhin, and Yudson.[7]

To summarize this section, we emphasize that all the spectra observed are well described by the knowledge of the dispersion relation of the surface-phonon polariton. The general shape of the dispersion relation corresponds to the dispersion relation for a flat surface. Yet, due to the interaction with the grating, the experimental dispersion relation shows branches unexpected from a simple folding of the flat surface dispersion relation. A numerical simulation of the dispersion relation based on a volume integral equation that fully accounts for the grating structure agrees within 0.1%. The dispersion relation obtained from the emission spectra is slightly different from the simulation. The discrepancy is attributed to the variation of the optical index with temperature that was not accounted for in the calculation.

D. Coherence of the thermal emission

In their paper on thermal emission by a grating, Wang and Zemel have shown that there is fair agreement between a numerical simulation of the absorptivity of a plane wave and experimental thermal emission spectra. They have argued that since the absorptivity was computed for a coherent incident wave, there must be some coherence in the thermal emission.[10] In our opinion, this argument does not provide any further information than Kirchhoff's law, which states that the directional monochromatic absorptivity is equal to the directional monochromatic emissivity. Yet the thermal emission of a grating can be partially spatially coherent. In the following, we discuss in more detail the issue of coherence in the context of thermal emission by a material supporting a surface wave.

1. Spatial coherence

First of all, it is necessary to recall the basic concepts of coherence theory. Coherence is a property of a given electromagnetic field denoted by $E(\mathbf{r}_1, t_1)$ (scalar approximation). It can be measured quantitatively using the concept of a mutual coherence function, which is essentially a correlation function of the field at two different points and two different times. This concept is useful for a random field. If the field is a microwave beam emitted by a well-controlled oscillator, its phase is deterministic. Its spatial coherence length is given by its spatial extension and its spatial coherence time is the emission time duration. Hence, the correlation function is not very useful in this context. The concept of coherence is more interesting when dealing with waves produced by sources with some degree of randomness such as a hot body. In this case the correlation function $\Gamma(\mathbf{r}_1, \mathbf{r}_2, t_1 - t_2)$ has to be evaluated in the sense of an average over an ensemble of realizations of the field:

$$\Gamma(\mathbf{r}_1, \mathbf{r}_2, t_2 - t_1) = \langle E(\mathbf{r}_1, t_1) E^*(\mathbf{r}_2, t_2) \rangle, \quad (5.1)$$

where the brackets denote the ensemble average and $*$ the complex conjugate. The above correlation function is known as the mutual coherence function. In Eq. (5.1) we have assumed that the fields are well described by a stationary random process so that the correlation function does depend only on $t_2 - t_1$. A difference can be made between spatial and temporal coherence. In simple terms, the temporal coherence characterizes the correlation of a field at a given point and different times. It is given by the ''equal point'' correlation function $\Gamma(\mathbf{r}, \mathbf{r}, t_1 - t_2)$. The spatial coherence characterizes the correlation of the field at different points and at the same time and is measured by $\Gamma(\mathbf{r}_1, \mathbf{r}_2, 0)$.

An important property of the temporal coherence is its connection with the spectral content of the field. This is given by the Wiener-Khinchin theorem. It states that the time correlation function $\Gamma(\mathbf{r}, \mathbf{r}, t_1 - t_2)$ is the Fourier transform of the power spectral density of the field. Thus, the width of the spectrum of the field is inversely proportional to the coherence time. In this respect, a blackbody appears to be a source producing a field with a very low temporal coherence. Conversely, a laser has a narrow frequency bandwidth so that the correlation time is large.

The simple idea to retain from this short discussion is that a source with a narrow peak in its frequency spectrum has some relatively long temporal coherence. A similar property exists for spatial coherence. Let us focus on the spatial properties of monochromatic fields by introducing the cross spectral density $W(\mathbf{r}_1, \mathbf{r}_2, \nu)$, which is the Fourier transform of the mutual coherence function $\Gamma(\mathbf{r}_1, \mathbf{r}_2, t)$ with respect to the variable t. $W(\mathbf{r}_1, \mathbf{r}_2, \nu)$ is useful to measure the spatial correlation of a monochromatic field. It has been shown recently that the specific intensity $I((\mathbf{r}_1 + \mathbf{r}_2)/2, \mathbf{u}, \nu)$ (or radiance) at the point $(\mathbf{r}_1 + \mathbf{r}_2)/2$ and in the direction specified by the unit vector $\mathbf{u}$ is the Fourier transform of $W(\mathbf{r}_1, \mathbf{r}_2, \nu)$ (Refs. 33 and 34) with respect to the space variable $\mathbf{r}_1 - \mathbf{r}_2$.

$$I(\mathbf{r}, \mathbf{u}, \nu) = \left(\frac{1}{\lambda}\right) \cos\theta \int \int W\left(\rho - \frac{\rho'}{2}, \rho + \frac{\rho'}{2}, \nu\right)$$
$$\times \exp\left(-i\frac{\omega}{c}\mathbf{u}\rho'\right) d\rho'. \quad (5.2)$$

This relation provides a theoretical foundation for the specific intensity, a concept that was introduced in the framework of the phenomenological theory of radiometry. Note the parallel between the Wiener-Khichin theorem and the above expression. In both cases, we deal with the Fourier transform of the mutual coherence function. The time Fourier transform gives the power spectral density and the space Fourier transform yields the specific intensity.

Since we are dealing with monochromatic light propagating in vacuum, the wave vector can be written as $(\omega/c)\mathbf{u}$ where $\mathbf{u}$ is the unit vector along the propagation direction. This result is essential to discuss the directivity of a partially coherent source. In simple words, if the correlation length of the field along a plane close to the source just above the source is large, the energy is emitted in a narrow cone. The directivity of the source increases with its spatial coherence. Experimental evidence of the property has been demonstrated by a number of groups.[35–38] Let us apply this result to the case of a thermal source. It is usually assumed that dif-

ferent points of a thermal source are not correlated. The coherence length is null and it turns out that such a source emits light in all directions.

The two simple rules of thumb that we have to keep in mind are (i) a peak in the frequency spectrum of the source implies the presence of some temporal coherence and (ii) a peak in a well-defined spatial direction implies the presence of some spatial coherence in the source.

2. Surface waves and partially spatially coherent emission

Let us now analyze the thermal emission at an interface in the presence of a surface wave. We assume that we detect the light emitted at a well-defined frequency by means of an interferential filter, for instance. The surface waves propagating along the interface are thermally excited with a well-defined wave-vector modulus. Therefore, due to these surface waves, the field along the interface is spatially correlated. The surface wave yields a periodic contribution to the cross spectral density. Therefore the specific intensity, which is its Fourier transform, has a peak at some angle. This behavior was not observed in our experiments because we have worked in a frequency region where the dispersion relation is almost flat ($d\omega/dk_\parallel = 0$). However, such a peak has been observed by Hesketh, Zemel, and Gebhart[9] who studied the thermal emission by a grating on doped silicon. A peak has also been observed for thermal emission by ZnSe by Vinogradov, Zhizhin, and Yudson.[7] These peaks in the angular behavior of the emissivity are a clear signature of the spatial coherence of the field along the interface that is induced by the propagation of the surface wave. We may wonder how a thermal source can produce a field with spatial coherence. For the usual surfaces, the thermally excited field is often considered as δ correlated.[39] To answer this question, it is necessary to go back to the physics of the surface-phonon polariton. A phonon is a collective excitation of the atoms of the material. This is the root of the coherence. A surface-phonon polariton is a phonon coupled to an electromagnetic wave. To some extent, one can say that the electromagnetic field receives the phonon coherence. The presence of angular peaks in the thermal emission can be understood as the result of interferences between the light scattered by different ridges illuminated by the same surface-phonon polariton propagating along the interface.

A similar analysis can be done for the temporal coherence. The presence of peaks in the frequency spectrum is a signature of the temporal coherence of the field on the interface. This coherence time is essentially the lifetime of the collective excitation.

To conclude this analysis, we put forward that the propagation of a monochromatic surface wave along the interface produces a partial spatial coherence of the electromagnetic field along the interface. This spatial coherence manifests itself in the directivity of the emitted intensity. This effect is a consequence of the presence of a surface wave that can be coupled if there is a grating. Thus it could also be observed in p polarization for an interface supporting a surface-plasmon polariton. It could also be seen for both polarizations in the case of guided waves in a dielectric film deposited on an opaque substrate. Conversely, for a given angle, the emission spectrum displays some narrow peaks that are the signature of the surface modes. Therefore, by applying

the Wiener-Khinchin theorem, a time correlation function could be deduced.

Let us conclude this section by discussing the difference between the results obtained in this paper and the results reported by Wang and Zemel. The thermal emission at a fixed frequency displays angular peaks in their results whereas we have not observed a peak with our SiC grating (see Fig. 8) for the directional absorptivity. The reason for this apparent discrepancy is due to the shape of the dispersion relation $d\omega/dk$. For a given detection bandwidth $\Delta\omega$, the spatial bandwidth is given by $\Delta\omega(dk/d\omega) = \Delta k$. If the dispersion relation has a large slope $d\omega/dk$, it turns out that a narrow part of the SPP is selected. The corresponding field is therefore spatially coherent. By contrast, if the slope $d\omega/dk$ tends to zero (as it does for our SiC grating in the spectral region studied, see Figs. 13 and 14), a large part Δk of the spectrum of the SPP is excited and the corresponding field has a low coherence length.

3. An alternative picture of spatially coherent thermal emission

Let us now provide a naive but useful picture of the thermal emission that also allows one to account for the coherence effects. Let us start by reasoning with a monochromatic plane wave that impinges on a flat interface separating a vacuum from a semi-infinite absorbing medium. In the framework of physical optics, one defines the reflectivity and the transmittivity by the Fresnel formulas. It turns out that the transmitted light will be absorbed so that the transmittivity of optical physics is the absorptivity of heat transfer theory. Invoking Kirchhoff's law (i.e., directional spectral emissivity and absorptivity are equal), it appears that the emissivity is the Fresnel transmittivity. This makes sense since one can interpret the emission by a surface as being a transmission process. Indeed, let us assume that the body is in equilibrium and that the radiation is well described by Planck's law within the material, then the *emitted* radiation is the equilibrium radiation *transmitted* by the interface.

At this point, one can remark that if a surface wave exists, there is a pole in the transmission factor. Therefore, there will be peaks of transmittivity for some particular directions and for particular frequencies corresponding to this pole. Thus, the transmission increases the coherence. We are back to the issue of the modification of the radiation coherence due to either transmission or reflection. This has been fully discussed recently in the case of reflection by a dielectric slab by Wang, Simon, and Wolf.[40] This picture also leads to the conclusion of the previous section. Any interface supporting a surface wave has a pole in its transmission factor. Therefore, it produces thermally emitted fields that are partially spatially coherent.

VI. SUMMARY AND CONCLUDING REMARKS

Monochromatic thermal emission by a grating supporting surface wave has unusual features. The field emitted in a given direction presents peaks at well-defined frequencies. Conversely, the field emitted at a fixed frequency may have peaks for some angles of emission. These effects are the consequence of the interplay between the periodicity of the surface and the presence of a thermally excited surface wave. Thus a complete analysis of the phenomenon requires a good

modeling of the propagation of a surface wave along a grating. Since the experimental pioneering work of Hesketh, Zemel, and Gebhart,[3] some progress has been made in the physics of surface waves and more recently on the issue of the propagation of surface waves along deep gratings. In order to fully account for the presence of the peaks, it is necessary to know the dispersion relation of the surface wave. We have studied experimentally the dispersion relation of a surface-phonon polariton using both the emission spectrum and the reflectivity spectrum. To our knowledge, this is the first measurement of a dispersion relation of a surface-phonon polariton along a grating using thermal emission.

Our numerical simulation matches the dispersion relation obtained from the reflectivity spectrum with an agreement better than 0.3%. It is a major result of this paper showing that today existing tools allow one to quantitatively describe these phenomena.

Finally, we have discussed the fundamental issue of coherence of the thermally emitted radiation. We have used the concepts of the coherence theory to provide a general framework that allows one to fully interpret the experimental results. In particular, we have shown that the existence of peaks in some angular directions implies that the field is partially coherent along the interface. We have discussed the role of the surface wave in this respect. From this discussion, it appears that any system supporting a surface wave such as a surface-plasmon polariton or a guided mode can emit partially spatially coherent light.

---

*Electronic address: janig@mail.atlantic-line.fr

†Present address: Commissariat à l'Énergie Atomique/LETI 38000 GRENOBLE.

‡Electronic address: jjg@em2c.ecp.fr

[1] P. J. Hesketh, B. Gebhart, and J. N. Zemel, J. Heat Transfer **110**, 680 (1988).

[2] P. Demont, M. Huetz-Aubert, and H. Tran N'Guyen, Int. J. Thermophys. **3**, 335 (1982).

[3] P. J. Hesketh, J. N. Zemel, and B. Gebhart, Nature (London) **325**, 549 (1986).

[4] H. Raether, *Surface Plasmons on Smooth and Rough Surfaces and on Gratings* (Springer-Verlag, Berlin, 1988).

[5] *Surface Polaritons*, edited by V. M. Agranovich and D. L. Mills (North-Holland, Amsterdam, 1982).

[6] *Electromagnetic Surface Modes*, edited by A. D. Boardman (John Wiley, New York, 1982).

[7] E. A. Vinogradov, G. N. Zhizhin, and V. I. Yudson, in *Surface Polaritons* (Ref. 5).

[8] P. J. Hesketh and J. N. Zemel, Phys. Rev. B **37**, 10 795 (1988).

[9] P. J. Hesketh, J. N. Zemel, and B. Gebhart, Phys. Rev. B **37**, 10 803 (1988).

[10] T. K. Wang and J. N. Zemel, Infrared Phys. **32**, 477 (1991).

[11] T. K. Wang and J. N. Zemel, Appl. Opt. **31**, 732 (1992).

[12] *Electromagnetic Theory of Gratings*, edited by R. Petit (Springer-Verlag, Berlin, 1988).

[13] L. Li, J. Opt. Soc. Am. A **11**, 2829 (1994).

[14] L. Li, J. Opt. Soc. Am. A **11**, 2816 (1994).

[15] A. Sentenac and J. J. Greffet, J. Opt. Soc. Am. A **9**, 996 (1992).

[16] B. Laks, D. L. Mills, and A. A. Maradudin, Phys. Rev. B **23**, 4965 (1981).

[17] A. A. Maradudin, in *Surface Polaritons* (Ref. 5).

[18] R. Ruppin, Solid State Commun. **8**, 1129 (1970).

[19] K. L. Kliewer and R. Fuchs, Phys. Rev. **144**, 495 (1966).

[20] W. G. Spitzer, D. Kleinman, and J. Walsh, Phys. Rev. **113**, 127 (1959).

[21] A. A. Maradudin, in *Surface Polaritons* (Ref. 5).

[22] P. Halevi, in *Electromagnetic Surface Modes*, edited by A. D. Boardman (Wiley, New York, 1982).

[23] E. T. Arakawa, M. W. Williams, and R. H. Ritchie, Phys. Rev. Lett. **31**, 1127 (1973).

[24] K. L. Kliewer and R. Fuchs, Adv. Chem. Phys. **27**, 355 (1974).

[25] T. C. Paulick, Phys. Rev. B **42**, 2800 (1990).

[26] M. Balkanski, in *Optical Properties of Solids*, edited by F. Abeles (North-Holland, Amsterdam, 1972).

[27] A. Wirgin, Opt. Acta **28**, 1377 (1981).

[28] J. Le Gall, P. Guinet, M. Olivier, and J. Y. Le Bris, J. Phys. (Paris) **4**, 651 (1994).

[29] H. P. Bates, in *Progress in Optics* (North-Holland, Amsterdam, 1976), Vol. XIII.

[30] H. C. Hottel and A. F. Sarofim, *Radiative Transfer* (McGraw-Hill, New York, 1967).

[31] D. L. Mills, Phys. Rev. B **15**, 3097 (1977).

[32] J. L. Stehle, O. T. Thomas, J. P. Piel, P. Evrard, J. H. Lecat, and L. C. Hammond, in *Polymer Based Molecular Composites*, edited by D. W. Schnefer and J. E. Mark, MRS Symposia Proceedings No. 171 (Materials Research Society, Pittsburgh, 1990), p. 349.

[33] L. Mandel and E. Wolf, *Optical Coherence and Quantums Optics* (Cambridge University Press, Cambridge, 1995).

[34] E. Wolf, Opt. Lett. **19**, 2024 (1995).

[35] P. De Santis, F. Gori, G. Guattari, and C. Palma, Opt. Commun. **28**, 256 (1979).

[36] F. Scudieri, M. Bertolotti, and R. Bartolino, Appl. Opt. **13**, 181 (1974).

[37] D. Courjon, J. Bulabois, and W. H. Carter, J. Opt. Soc. Am. **71**, 469 (1981).

[38] E. Tervonen, A. T. Friberg, and J. Turunen, J. Opt. Soc. Am. A **9**, 796 (1992).

[39] L. D. Landau and E. M. Lifshitz, *Electrodynamics of Continuous Media* (Pergamon, Oxford, 1960).

[40] W. Wang, R. Simon, and E. Wolf, J. Opt. Soc. Am. A **9**, 287 (1992).